

**RECOMMENDATIONS FOR DESIGN OF POST-TENSIONED  
SLAB-COLUMN CONNECTIONS SUBJECTED TO LATERAL  
LOADING**

By

THOMAS H.-K. KANG, IAN N. ROBERTSON, NEIL M.  
HAWKINS,  
AND JAMES M. LAFAVE



Authorized reprint from: February 2008 issue of the PTI Journal

Copyrighted © 2008, Post-Tensioning Institute

# RECOMMENDATIONS FOR DESIGN OF POST-TENSIONED SLAB-COLUMN CONNECTIONS SUBJECTED TO LATERAL LOADING

THOMAS H.-K. KANG, IAN N. ROBERTSON, NEIL M. HAWKINS,  
AND JAMES M. LAFAVE

## ABSTRACT

A detailed review on lateral load tests of post-tensioned concrete slab-column connections and frames is conducted. Key geometric parameters, boundary and loading conditions, and the observed responses of the test specimens are all documented. Based on a review of this database of tests, a series of design recommendations are suggested for post-tensioned slab-column connections that are part of non-participating frames, as well as part of intermediate moment frames. These design recommendations include: (1) lateral drift capacity, (2) maximum allowable gravity shear, (3) punching shear strength, and (4) reinforcement details.

## KEYWORDS

concrete; slab-column connection; flat plate; post-tensioning; post-tensioned concrete; shear reinforcement; drift capacity; punching shear capacity; anchorage, roof joints; lateral loading; seismic; earthquake.

## INTRODUCTION & BACKGROUND

Slab-column frames of structural concrete are commonly used to carry gravity loads in regions of high seismicity as so-called “non-participating” frames, where all design lateral force demands are intended to be taken by moment resisting frames or structural walls. Where such slab-column frames are assigned to high seismic performance category structures and are not considered to contribute to lateral resistance, the lateral drifts for the frames may need to be controlled to avoid punching failures, associated with the Life Safety condition, at the slab-column connections during inelastic lateral deformations. Because no provisions have traditionally existed regarding the proportioning of non-participating slab-column frames, Section 21.11 of ACI 318-05<sup>1</sup> entitled “Members not designated as part of the lateral-force-resisting system”, was revised and updated for the 2005 code to address concerns regarding the lateral drift capacities of slab-column connections.

In Section 21.11.5 of ACI 318-05<sup>1</sup> new design criteria for the use of shear reinforcement at slab-column connections were defined, based primarily on a database of test results for reinforced concrete (RC) slab-column connections (Moehle,<sup>2</sup> Megally and Ghali<sup>3</sup>). These ACI criteria are a function of the relationship between the lateral-load drift capacity at punching of slab-column connections and the gravity shear ratio ( $V_u/\phi V_c$ ) acting on the connection.  $V_u$  is the factored gravity shear force determined per the load combinations specified in ACI 318-05<sup>1</sup> Section 21.11.5,  $\phi$  is 0.75 per ACI 318-05<sup>1</sup> Section 9.3.2.3, and  $V_c$  is the nominal concrete shear strength per ACI 318-05<sup>1</sup> Section 11.12.2.

The Section 21.11.5 provisions for non-participating slab-column frames define the design story drift capacity at punching, associated with the Life Safety condition, as equal to  $[0.035 - 0.05(V_u/\phi V_c)]$  for  $V_u/\phi V_c$  less than 0.6, and as 0.005 for larger gravity shear ratios (see Fig. 1). This drift capacity must be greater than the computed design story drift ratio (drift demand); otherwise, designers should demonstrate that the design shear and induced moment at the design story drift can, in fact, be transferred. If this deformation compatibility requirement is not met, then use of shear reinforcement, or possibly re-design

---

PTI Journal, V. 6, No. 1, February 2008 Received and reviewed under Institute Journal publication policies. Copyright ©2008, Post-Tensioning Institute. All rights reserved, including the making of copies unless permission is obtained from the Post-Tensioning Institute. Pertinent discussion will be published in the next issue of the PTI Journal if received within 3 months from the publication.

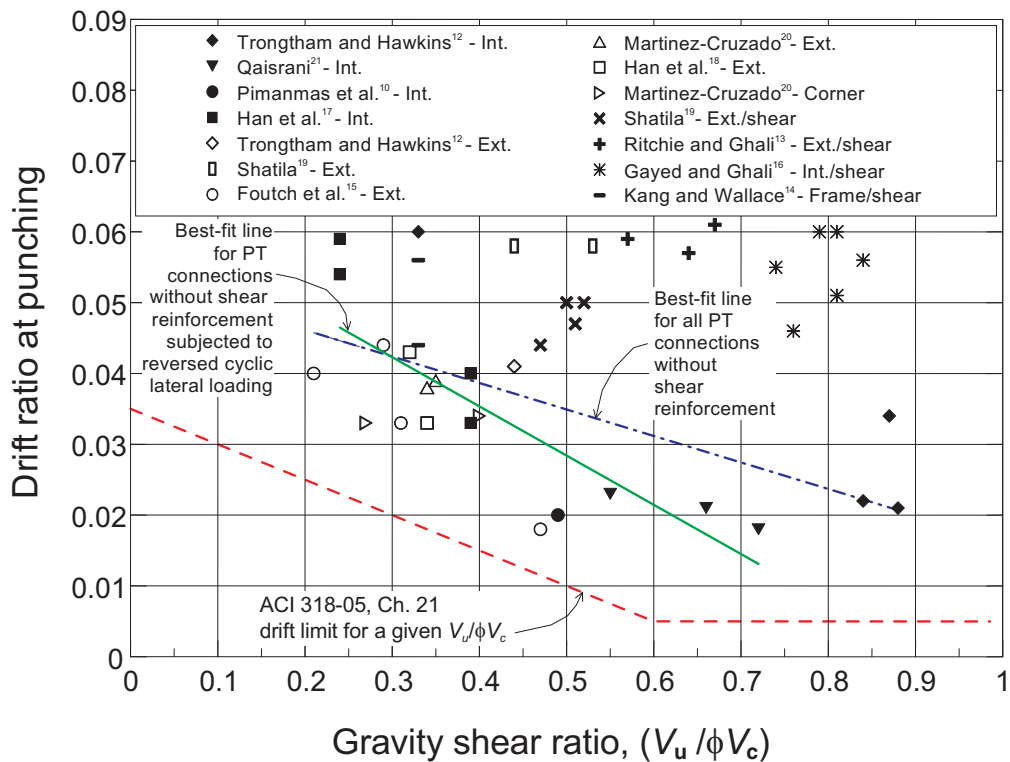


Fig. 1 - Drift ratio at punching versus gravity shear ratio for post-tensioned slab-column connections with and without shear reinforcement, where  $V_c$  is defined in accordance with ACI 318-05, Eq. (11-36)

of the members, is necessary. Shear reinforcement with specified strength and extension may also be used instead of even making this deformation compatibility check. Shear reinforcement is often required if the seismic-force resisting system (SFRS) is a special moment frame or a high-rise special structural wall. Shear reinforcement may not be required if the SFRS is a low-to-mid-rise special structural wall, which tends not to produce drifts greater than the ACI drift limit for slab-column connections.

Subcommittees of ACI Committee 374, Performance-Based Seismic Design of Concrete Buildings, and Joint ACI-ASCE Committee 352, Joints and Connections in Monolithic Concrete Structures, have recompiled and expanded the database of test results and reassessed these data to recommend lateral drift limits for the various performance levels as a function of the gravity shear ratio,  $V_u/\phi V_c$  (Hueste et al.<sup>4</sup>). For the test data,  $V_u$  is the experimentally determined gravity load shear force acting at the critical section of the slab for two-way action,  $\phi = 1.0$ , and  $V_c$  is calculated per Eq. (11-36) of ACI 318-05.<sup>1</sup>

The newly-compiled data set includes test results for more than 70 conventionally reinforced concrete slab-column connection specimens fabricated with and without shear reinforcement (Pan and Moehle,<sup>5</sup> Moehle,<sup>2</sup> Hueste and

Wight,<sup>6</sup> Megally and Ghali,<sup>3</sup> Robertson et al.,<sup>7</sup> Kang and Wallace<sup>8</sup>). The data set shows that the ACI 318-05<sup>1</sup> drift limit (Section 21.11.5(a)) for determining the need for shear reinforcement represents the lower bound of the drift ratios at sudden punching or a drop to 80% of the peak lateral load. Only 4 of 76 test data points fall slightly below the ACI limit. None of the results in that data set, however, are for post-tensioned (PT) slab-column connections.

Given the widespread use of PT flat plate systems in the U.S., investigation of the seismic performance of PT slab-column connections and the development of seismic design provisions for such systems is needed. Joint ACI-ASCE Committee 352 is therefore currently revising ACI 352.1R-89<sup>9</sup> *Recommendations for Design of Slab-Column Connections in Monolithic Reinforced Concrete Structures*, to address this need. As part of that effort, a detailed review has been conducted of all research currently available on lateral load tests of PT slab-column connections. Particular emphasis has been placed on the lateral drift capacity as a function of the gravity shear ratio. The predicted punching shear capacity of PT connections using the eccentric shear stress model has also been investigated. Further, seismic detailing issues for shear reinforcement and column bar anchorage inside roof slab-column joints have been reviewed. A summary of the detailed review follows.

## SUMMARY OF AVAILABLE RESEARCH

Table 1 summarizes the existing experimental data on lateral load tests of PT slab-column connections with and without shear reinforcement. For connections without shear reinforcement, the database of available tests includes twelve interior, eleven exterior, and two corner connections. For connections with shear (headed studs) reinforcement, the existing tests consist of six interior and seven exterior connections, and a two-story, two-bay by two-bay frame.

Three different arrangements of slab post-tensioning tendons were used in the specimens (Table 1), including: (1) Banded tendons in the lateral loading direction and Distributed tendons in the other direction (B-D); (2) Distributed tendons in the loading direction with Banded tendons in the other direction (D-B); and (3) Distributed tendons in both directions (D-D). The classification is based on the direction of first applied lateral loading for the few connections subjected to biaxial lateral loading. While a configuration with distributed tendons in both directions was often used in the early days of PT slabs, most current construction uses banded tendons in one direction. All specimens had tendons draped in a parabolic profile and placed through the column cages, except for the one specimen tested by Pimanmas et al.,<sup>10</sup> where tendons were placed in a straight profile at the top of the slab and no tendons were placed through the column. Square columns were used in all specimens except for the connection tested by Pimanmas et al.,<sup>10</sup> where a rectangular column cross-section was selected to provide greater stiffness in the moment transfer direction.

In all specimens, slab top bonded conventional reinforcing bars were placed around the connection, per Section 18.9 of ACI 318-05<sup>1</sup> and Section 5.3.3.3 of the Post-Tensioning Manual,<sup>11</sup> to ensure flexural continuity and to limit crack widths and spacing. Bottom bonded reinforcement was provided in nearly two-thirds of the specimens. Of those specimens, nine (Trongtham and Hawkins,<sup>12</sup> Ritchie and Ghali,<sup>13</sup> and Kang and Wallace<sup>14</sup>) had almost the same amount of conventional bottom reinforcement as top reinforcement within an effective transfer width of  $c_2 + 3h$ , while seventeen (Foutch et al.,<sup>15</sup> Pimanmas et al.,<sup>10</sup> Gayed and Ghali,<sup>16</sup> and Han et al.<sup>17,18</sup>) included bottom bars with less than two-thirds of the area of the top bars. Here  $c_2$  is the column dimension perpendicular to the moment transfer direction and  $h$  is the slab thickness.

In Table 1, the actual gravity shear ratios ( $V_u/\phi V_c$ ) are tabulated based on as-measured direct shear forces and material properties. Since the material properties and geometries used in the expression for  $V_c$  are measured values for all test specimens, the appropriate  $\phi$  factor for these data is unity. Twenty four of the 39 specimens were tested under Constant Gravity load (CG) that was unchanged throughout the duration of the test. For the rest of the specimens, however, the gravity shear force on the connection was

increased at specific times during the test. Therefore, only the Gravity shear ratio at Punching (GP) has been reported in those cases, allowing an equal basis for comparison. For all of these PT connections,  $V_c$  is calculated using the provisions of ACI 318-05,<sup>1</sup> Section 11.12.2.2 and Post-Tensioning Manual,<sup>11</sup> Section 5.4.3. That is,  $V_c = (\beta_p \sqrt{f'_c} + 0.3f_{pc})b_0d + V_p$  (lbs), where  $\beta_p$  is the smaller of 3.5 and  $(\alpha_s d/b_0 + 1.5)$ , with  $\alpha_s = 40, 30$  and  $20$  for interior, exterior and corner connections, respectively, and  $b_0$  is the perimeter of the assumed critical section (in.),  $d$  is the effective depth (in.),  $f'_c$  is the concrete compressive strength (psi),  $f_{pc}$  is the average compressive stress in concrete due to the effective post-tensioning force for the full specimen width (psi), and  $V_p$  is the vertical component of all effective post-tensioning forces crossing the critical section. However, the last term ( $V_p$ ) was ignored because the angle of tendon inclination was small for all PT slabs and the tendons were essentially horizontal as they crossed the critical section for shear.

The effective depth ( $d$ ) was taken as the average of the effective depths ( $d_p$ ) of tendons or bonded bars in the two directions. For exterior connections,  $d$  was set equal to  $d_p$  for the tendons parallel to the slab edge. Note that, for exterior connections transferring moments normal to the slab edge, the tendons in the direction perpendicular to the edge were vertically centered in the slab. To be consistent with the other test data and the approach taken by most researchers, the value of the gravity shear ratio ( $V_u/\phi V_c$ ) reported by Pimanmas et al.<sup>10</sup> was modified using the average  $d_p$  in the two directions rather than the  $d_p$  value for the tendons in the moment transfer direction only. The outer diameter of the tendons, taken as including the plastic tubes sheathing the prestressing steel, in this reduced-scale specimen was large relative to the slab thickness. Therefore, the modified calculation of  $d_p$  led to a significant change in  $V_u/\phi V_c$ —from a reported value of 0.28 to a value of 0.49 in the current database.

The increase in computed shear strength due to the in-plane compression ( $f_{pc}$  of generally 150 to 250 psi; 1.0 to 1.7 MPa) typically results in a shear strength about 5 to 15% greater than that of an equivalent reinforced concrete connection without post-tensioning. For the purpose of this study, the limits of ACI 318-05,<sup>1</sup> Sections 11.12.2.2(a), (b), and (c), respectively, concerning the distance from the column perimeter to the slab edge, the maximum value of  $\sqrt{f'_c}$ , and the limits on  $f_{pc}$  were ignored.

Most of the tests were conducted on isolated connection subassemblies (Fig. 2) at approximately one-half to two-thirds scale, with the slab edges being pin-supported along assumed lateral load inflection points (i.e. at or near the slab mid-spans); see Fig. 2(b) and 2(d). These isolated specimens had columns extending above and below the slab for a total distance equal to the story height, and the columns were displaced laterally during testing to produce

Table 1 - Post-tensioned slab-column connections subjected to lateral loading

Specimens		Joint Type (3)	Tendon layout (4)	Gravity loads (5)	$\phi V_c$ kips (6)	$V_u$ kips (7)	$\frac{V_u}{\phi V_c}$ (8)	$f_c$ psi (9)	$f_{pc}$ psi (10)	$b_0$ in. (11)	$d$ in. (12)	$h$ in. (13)	$I_1^{\dagger\dagger}$ in. (14)	Lateral loads (15)	DR % (16)
Trongtham and Hawkins <sup>12</sup>	S1	Int	B-D	GP	79.6	66.8	0.84	3900	163	73	4.1	5.5	222	RPL	2.2
	S2	Ext	D-D	GP	69.3	30.8	0.44	4200	277	51	4.4	5.5	252	RPL	4.1
	S3	Int	D-B	GP	77.9	67.8	0.87	3698	163	73	4.1	5.5	222	RPL	3.4
	S4	Int	D-D	GP	79.2	69.9	0.88	3800	163	73	4.1	5.5	222	RPL	2.1
	S5	Int	D-D	GP	77.4	25.2	0.33	3596	163	73	4.1	5.5	222	RPL	6.0
Shatila <sup>19</sup>	S1	Ext	B-D	GP	76.2	40.5	0.53	5188	540	39	4.7	5.9	99	RPL	5.8
	S2 <sup>†</sup>	Ext	B-D	GP	78.4	40.5	0.52	5710	540	39	4.7	5.9	99	RPL	5.0
	S3 <sup>†</sup>	Ext	B-D	GP	81.6	40.5	0.50	6072	570	39	4.7	5.9	99	RPL	5.0
	S4 <sup>†</sup>	Ext	B-D	GP	78.7	40.5	0.51	5783	540	39	4.7	5.9	99	RPL	4.7
	S5 <sup>*</sup>	Ext	B-D	GP	91.1	40.5	0.44	5986	570	44	4.7	5.9	99	RPL	5.8
	S6 <sup>†*</sup>	Ext	B-D	GP	86.6	40.5	0.47	5304	550	44	4.7	5.9	99	RPL	4.4
Foutch et al. <sup>15</sup>	S1	Ext	B-D	GP	61.6	13.0	0.21	7300	450	43	3.3	4.0	168	MTL	4.0
	S2	Ext	B-D	GP	60.8	18.7	0.31	6200	510	43	3.3	4.0	168	MTL	3.3
	S3	Ext	D-B	GP	52.4	15.1	0.29	6100	320	43	3.3	4.0	168	MTL	4.4
	S4	Ext	D-B	GP	55.0	25.6	0.47	7000	315	43	3.3	4.0	168	MTL	1.8
Martinez <sup>20</sup>	E1	Ext	D-B	CG	25.4	9.0	0.35	4800	199	29	2.9	3.6	144	RCL	3.9
	E2	Ext	B-D	CG	25.2	8.5	0.34	4620	206	29	2.9	3.6	144	RCL	3.8
	C1	Cor	B-D	CG	18.1	7.2	0.40	5890	223	18	2.9	3.6	144	RCL	3.4
	C2	Cor	D-B	CG	18.2	4.9	0.27	6130	211	18	2.9	3.6	144	RCL	3.3
Qaisrani <sup>21</sup>	I1	Int	D-B	CG	35.6	25.5	0.72	4075	240	43	2.8	3.5	147	RCL	1.8
	I2	Int	D-B	CG	35.6	23.5	0.66	4075	240	43	2.8	3.5	147	RCL	2.1
	I3	Int	D-B	CG	35.6	19.5	0.55	4010	240	43	2.8	3.5	147	RCL	2.3
Pimanmas et al. <sup>10</sup>		Int	B-D	CG	60.6	29.9	0.49	5858	240	70	2.8	4.7	224	RCL	2.0
Kang and Wallace <sup>14</sup>	PT Frame <sup>†</sup>	1 <sup>st</sup> story	B-D	CG	26.0	8.6	0.33	4012	200	41	2.3	3.0	112	RCL	4.4
		2 <sup>nd</sup> story	B-D	CG	26.0	8.6	0.33	4012	200	41	2.3	3.0	112	RCL	5.6
Ritchie and Ghali <sup>13</sup>	EC3C <sup>†</sup>	Ext	B-D	CG	36.9	24.7	0.67	3741	58	38	4.2	5.9	95	RCL	6.1
	EC5C <sup>†</sup>	Ext	B-D	CG	38.6	24.7	0.64	3712	95	38	4.2	5.9	95	RCL	5.7
	EC9C <sup>†</sup>	Ext	B-D	CG	43.4	24.7	0.57	4089	160	38	4.2	5.9	95	RCL	5.9
Gayed and Ghali <sup>16</sup>	IPS-3 <sup>†</sup>	Int	B-D	CG	64.0	54.0	0.84	3880	60	57	4.5	6.0	75	RCL	5.6
	IPS-5 <sup>†</sup>	Int	B-D	CG	67.0	54.0	0.81	4150	90	57	4.5	6.0	75	RCL	6.0
	IPS-5R <sup>†</sup>	Int	D-B	CG	66.0	54.0	0.81	4120	90	57	4.5	6.0	75	RCL	5.1
	IPS-7 <sup>†</sup>	Int	B-D	CG	73.0	54.0	0.74	4460	130	57	4.5	6.0	75	RCL	5.5
	IPS-9 <sup>†</sup>	Int	B-D	CG	71.0	54.0	0.79	3400	160	57	4.5	6.0	75	RCL	6.0
	IPS9R <sup>†</sup>	Int	D-B	CG	69.0	54.0	0.76	3730	160	57	4.5	6.0	75	RCL	4.6
Han et al. <sup>17</sup>	PI-B50	Int	B-D	CG	77.1	29.7	0.39	4684	175	64	4.1	5.1	189	RCL	3.3
	PI-B30	Int	B-D	CG	77.1	18.2	0.24	4684	175	64	4.1	5.1	189	RCL	5.9
	PI-D50	Int	D-B	CG	77.1	29.7	0.39	4684	175	64	4.1	5.1	189	RCL	4.0
	PI-D30	Int	D-B	CG	77.1	18.2	0.24	4684	175	64	4.1	5.1	189	RCL	5.4
Han et al. <sup>18</sup>	PE-B50	Ext	B-D	CG	55.7	18.9	0.34	4684	175	44	4.3	5.1	189	RCL	3.3
	PE-D50	Ext	D-B	CG	55.7	18.0	0.32	4684	175	44	4.3	5.1	189	RCL	4.3

Notes

Int = Interior; Ext = Exterior; Cor = Corner

$V_u$  = Direct shear force acting on the slab critical section for two-way action

$\phi V_c$  = Shear strength for test connection, calculated with  $\phi = 1.0$  and using  $V_c$  per Eq. (11-36) of ACI 318-05

<sup>†</sup> indicates specimens with shear reinforcement

<sup>††</sup> indicates slab span length of scaled-down prototype

\* indicates exterior connections with cantilevered slab overhangs

DR = Drift ratio at punching (for negative bending for exterior and corner connections)

DR =  $\Delta/l$  per Fig. 2(a) and 2(c)<sup>12,15</sup> (Ext connections tested by Trongtham and Hawkins<sup>12</sup> and Foutch et al.<sup>15</sup>)

DR =  $\frac{1}{2}(\Delta/l + \Delta/l)$  per Fig. 2(a). (Int connections tested by Trongtham and Hawkins<sup>12</sup>)

DR =  $\Delta/l_a$  per Fig. 2(b). (Connections tested by Shatila<sup>19</sup>)

DR =  $\Delta/l$  per Fig. 2(b). (Connections tested by Ritchie and Ghali<sup>13</sup> and Gayed and Ghali<sup>16</sup>)

DR =  $\Delta/l$  per Fig. 2(d). (Connections tested by Qaisrani<sup>21</sup>, Martinez-Cruzado<sup>20</sup>, Pimanmas et al.<sup>10</sup> and Han et al.<sup>17,18</sup>)

DR =  $\frac{1}{2}(\Delta/l_a + \Delta/l_b)$  for 1st floor connections and

DR =  $\Delta/l_b$  for 2nd floor connections per Fig. 2(e). (Connections tested by Kang and Wallace<sup>14</sup>)

Conversion: 1 in. = 25.4 mm; 1 kip = 4.45 kN; 1 psi = 0.0069 MPa

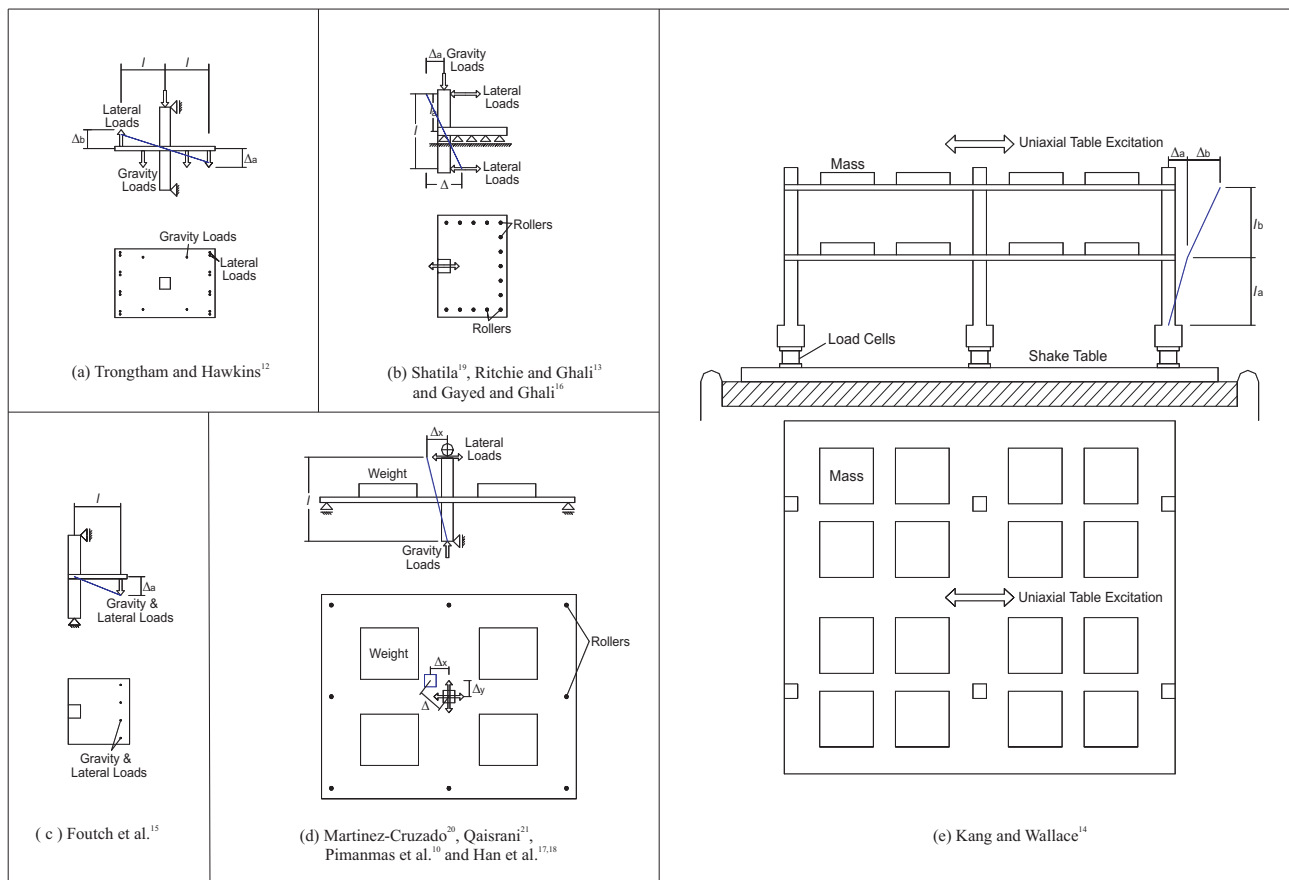


Fig. 2 - Typical test configurations (Scaled to have the same story height)

unbalanced moments at the slab-column connections. However, the models tested by Trongtham and Hawkins<sup>12</sup> and by Foutch et al.<sup>15</sup> represented reduced portions of the slabs surrounding the columns, as both the gravity and lateral loads were simulated by displacing the slabs (Fig. 2(a) and 2(c)). The slab span lengths  $l_1$  for these specimens were determined based on the actual (scaled-down) prototype buildings used for proportioning and constructing the specimens and are reported in Table 1.

The ratios of the slab span length (center-to-center of columns) to the slab thickness ( $l_1 / h$ ) used for most of the specimens ranged between 35 and 48, which are typical of values used for PT flat plate construction in the U.S. However, the tests conducted by Shatila,<sup>19</sup> by Ritchie and Ghali,<sup>13</sup> and by Gayed and Ghali<sup>16</sup> represented a significantly lower span-to-thickness ratio that was only about 15 (Fig. 2(b)). All of these ratios were computed assuming that inflection points would occur near the slab mid-spans when such slab-column frames are subjected to substantial lateral loads. The much lower values in some tests may better represent the case under high gravity loads when the slab inflection point would be nearer to the slab quarter span.

A variety of loading and boundary condition schemes were used in the tests by the different researchers, as depicted in Fig. 2. The types of lateral loads applied to the specimens are classified into three categories – MonoTonic lateral Loading (MTL), RePeated lateral Loading (RPL), and Reversed Cyclic lateral Loading (RCL). RPL means lateral loads that were cycled several times, but within the same bending direction. The two-story by two-bay frame (Kang and Wallace<sup>14</sup>) was tested using a shaking table to simulate earthquake actions (Fig. 2(e)). The specimens tested by Martinez-Cruzado<sup>20</sup> and by Qaisrani<sup>21</sup> (Fig. 2(d)) were subjected to clover-leaf patterns of biaxial lateral drift, with four quadrant loops in each cycle. Results for all these tests are also categorized as RCL.

### DRIFT CAPACITY AT PUNCHING VERSUS GRAVITY SHEAR RATIO

Assessments of the drift capacities at either sudden punching or when the lateral load had dropped to 80% of the peak lateral load were carefully conducted for each test program. The results are shown in Table 1 and Fig. 2. The resulting values of assessed drift capacity are essentially those associated with the life safety performance level because no



test resulted in complete collapse or complete loss of lateral load capacity, due to the presence of continuous tendons and/or bottom reinforcement through the column core.

For the tests performed by Trongtham and Hawkins<sup>12</sup> and by Foutch et al.,<sup>15</sup> the lateral drift ratio was determined as the slab edge deflection due to input slab deformations, divided by the length between the column centerline and the measured slab end point (Fig. 2(a) and 2(c)). For the interior connections (S1, S3, S4, and S5) tested by Trongtham and Hawkins,<sup>12</sup> the drift ratios on both sides of the column at punching were averaged (Table 1). For the tests carried out by Shatila,<sup>19</sup> and by Ritchie and Ghali<sup>15</sup> and Gayed and Ghali,<sup>16</sup> the drift ratios at punching were defined as  $(\Delta_2 / l_2)$  and  $(\Delta / l_c)$ , respectively, as shown on Fig. 2(b). For the rest of the reversed cyclic tests of isolated slab-column connections (Qaisrani,<sup>21</sup> Martinez-Cruzado,<sup>20</sup> Pimanmas et al., 2004,<sup>10</sup> and Han et al.<sup>17,18</sup>), the drift ratio was taken as the lateral displacement of the column top relative to the base of the column, divided by the column height (Fig. 2(d)).

Punching was noted at vector drift ratios for the specimens subjected to bi-axial loading (Qaisrani,<sup>21</sup> Martinez-Cruzado<sup>20</sup>), when a drift cycle in one direction was reached and a drift cycle in the other direction was underway. Note that even though drift ratios in two-way directions are considered for the connections subjected to bi-axial loading, ACI 318-05<sup>1</sup> does not require checking of the connection shear strength for bi-axial moment transfer. Rather a check is required for each principal direction of loading only, by using the eccentric shear stress model of ACI 318-05,<sup>1</sup> Section 11.12.6 (Concrete International<sup>22</sup>). For the dynam-

ic tests of the two-story PT slab-column frame (Kang and Wallace<sup>8,23</sup>), the drift ratios at punching were aggregately determined using the average of the inter-story drift ratios for the stories above and below a connection. Each floor level consisted of two interior and four exterior connections (Fig. 2(e)) having the same column and slab geometry, gravity load level, etc.

Relationships for drift capacity at punching versus gravity shear ratio for all the test results (39 specimens) are plotted in Fig. 1. The database indicates that the drift capacity at punching for PT slab-column connections is strongly influenced by the direct gravity shear ratio, as is also the case for reinforced concrete connections. Figure 1 further shows that the ACI 318-05,<sup>1</sup> Section 21.11.5 requirement for use of shear reinforcement in slab-column connections is conservative for PT connections, as has previously also been noted for conventional RC connections (Pan and Moehle,<sup>5</sup> Moehle,<sup>2</sup> Hueste and Wight,<sup>6</sup> Robertson et al.,<sup>7</sup> and Kang and Wallace<sup>8</sup>). The influence of gravity shear is especially evident for connections tested within a specific test program (e.g., for the series of tests by Trongtham and Hawkins,<sup>12</sup> Foutch et al.,<sup>15</sup> Qaisrani,<sup>21</sup> or Han et al.<sup>17,18</sup>).

The trend lines in Fig. 3 were derived from the databases of RC and PT specimens without shear reinforcement (Kang and Wallace<sup>8</sup>) using a linear least-squares fit method. The trend lines suggest that PT connections can sustain higher lateral drift ratios prior to punching than comparable RC connections (without shear reinforcement and under a variety of loading types). The higher drift capacities are in part due to the larger span-to-thickness ratios ( $l_1 / h$ ) used in PT slab-column construction (i.e., approximately 25 for RC

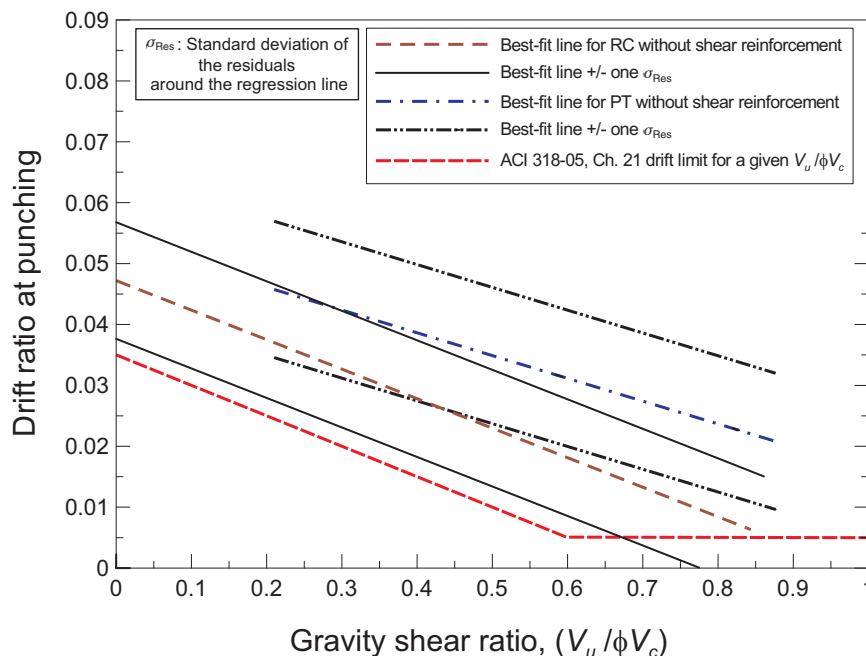


Fig. 3 - Best-fit lines and confidence bands for conventionally reinforced and post-tensioned slab-column connections, where  $V_c$  is defined in accordance with ACI 318-05, Eq. (11-33) through (11-36)  
 Note: Best-fit lines and standard deviations are based on the data only.

versus approximately 40 for PT). That increase makes PT slabs more flexible than RC slabs, in the light of the fact that a PT slab is likely to be less cracked.

The results also indicate that the range of loading conditions for the PT specimens without shear reinforcement, from monotonic to reversed cyclic, somewhat impacted the drift capacity at punching (Table 1; Fig. 1). The trend line for the fourteen PT specimens subjected to reversed cyclic loads results in somewhat lower drift ratio capacities than for all specimens and all loading conditions. Although some test results indicate that the tendon arrangement in the direction of moment transfer (distributed versus banded) could improve the drift capacity of the PT connection in that direction (e.g., Han et al.<sup>17,18</sup>), no significant differences in drift capacities at punching were noted as a function of the tendon arrangement across all PT specimens. Furthermore, because the PT data are somewhat limited, no distinction is made here in the drift capacity for the connection types (i.e., interior versus exterior). Similarly, no such distinction for connection type is currently made in ACI 318-05,<sup>1</sup> Section 21.11.5 even though some test data for RC

connections (Megally and Ghali<sup>3</sup>) show that drift ratio capacities are higher for exterior than interior connections.

Somewhat larger drift capacities at punching were observed for isolated PT exterior connections with shear reinforcement (e.g., Ritchie and Ghali<sup>13</sup>) relative to those without shear reinforcement (e.g., Martinez-Cruzado,<sup>20</sup> Han et al.<sup>18</sup>), as seen in Fig. 1. This result is probably due to the large strain ductility provided by yielding of shear reinforcement. However, a seemingly contrary result was found within the test program conducted by Shatila<sup>19</sup> (Table 1; Fig. 1). As mentioned earlier, the specimens tested by Shatila,<sup>19</sup> and by Ritchie and Ghali<sup>13</sup> and Gayed and Ghali<sup>16</sup> were proportioned to represent relatively low slab span-to-thickness ratios ( $l_1 / h$ ) on the order of about 15. Further, because they used rollers along all edges of the slab, (see Fig. 2(b)), the deformed shape of the slab could be inconsistent, across the slab width, with that in a real building. Such test configurations tend to induce larger slab shear-to-moment ratios at the slab-column interfaces than for typical flat plate geometric and boundary conditions. Compare, for example, Fig. 2(b) versus 2(d) or 2(e). Thus,

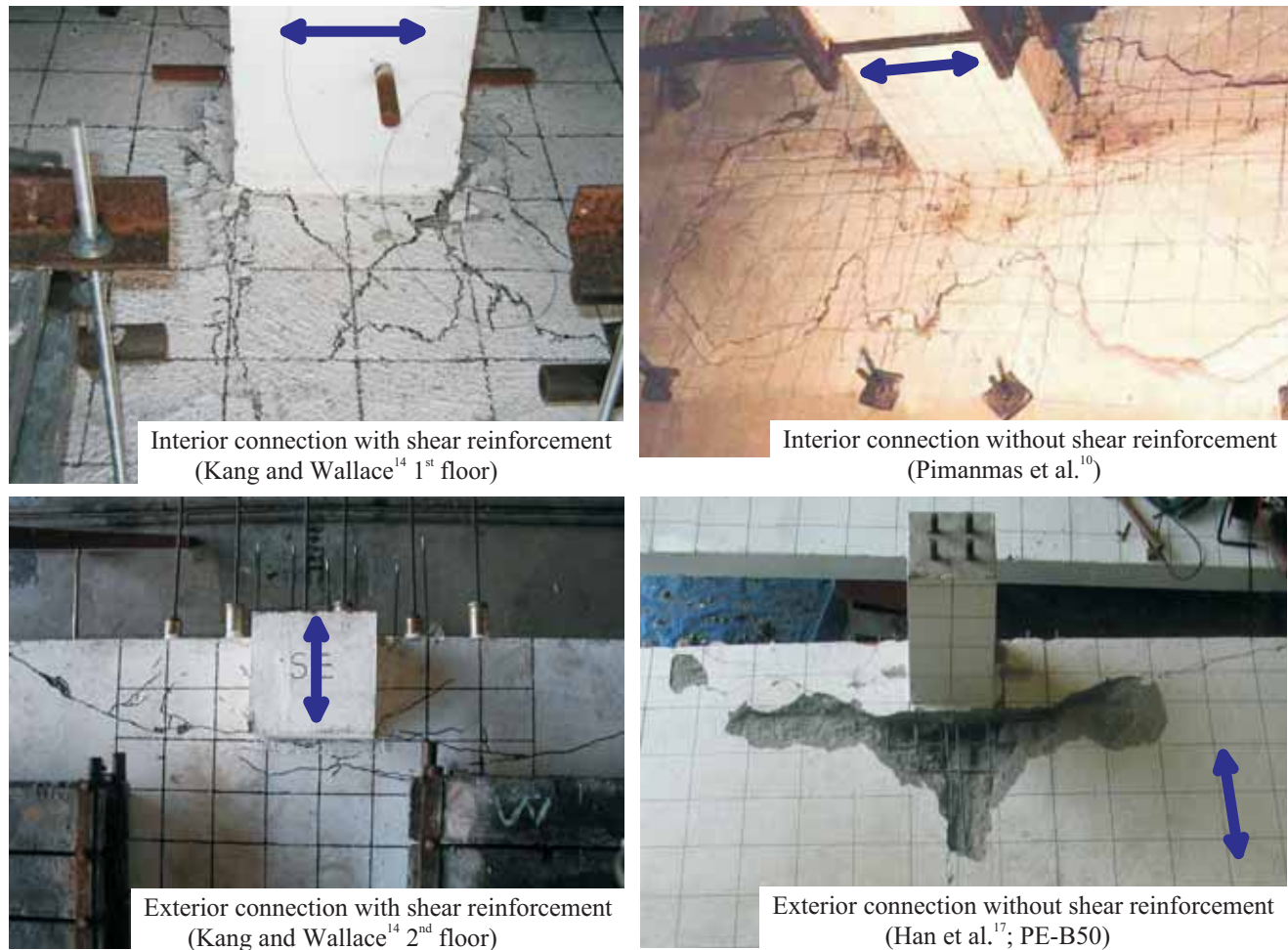


Fig. 4 - Observed punching damage after the tests (Arrows indicate testing directions)



these lateral drift results may not be appropriate for direct comparisons with other results for systems having greater span-to-thickness ratios.

The range of drift ratios at punching observed for the PT flat plate frames with shear reinforcement (Kang and Wallace<sup>14</sup>) is similar to that obtained for isolated PT connections without shear reinforcement, as indicated in Table 1 and Fig. 1. Although punching occurred at drift levels similar to those for connections without shear reinforcement, the use of shear reinforcement significantly reduced the extent of punching damage and the shear strength degradation after punching, as can be seen in Fig. 4. Most of the specimens without shear reinforcement (e.g.,

Martinez-Cruzado,<sup>20</sup> Qaisrani,<sup>21</sup> Pimanmas et al.,<sup>10</sup> Han et al.<sup>17,18</sup>) experienced sudden punching failures and had very low residual strengths, typically only 20 to 30% of the peak lateral load (Fig. 5(a) and 5(b)). On the other hand, specimens with shear reinforcement (e.g., Ritchie and Ghali,<sup>13</sup> Kang and Wallace<sup>14</sup>) exhibited only gradual strength degradation after reaching the peak lateral load. Residual strengths after punching were often greater than 60% of the peak lateral load, even after several post-punching loading cycles to increasing drift ratios (Fig. 6(a) and 6(b)).

The lateral drift capacity of connections was not significantly affected by the presence of bottom reinforcing bars; however, the energy dissipation was increased. For PT con-

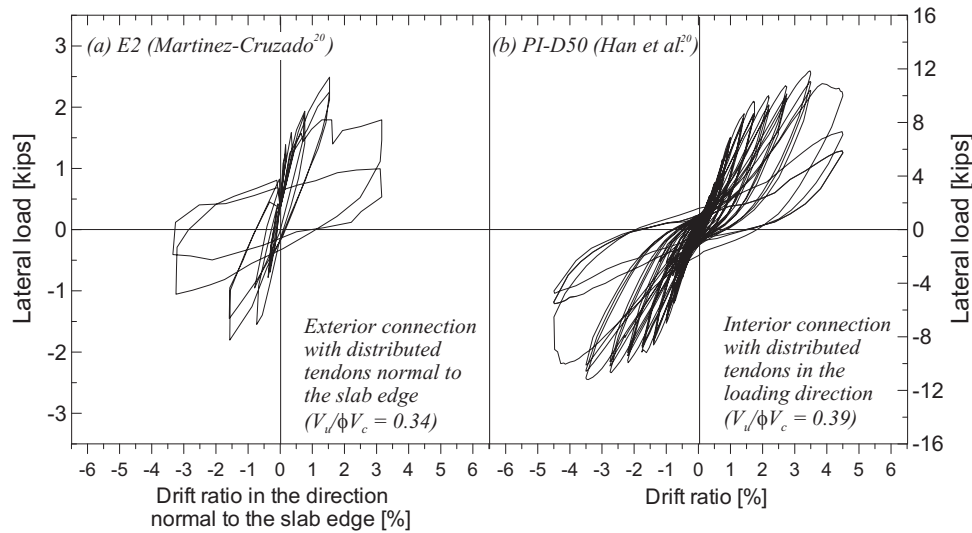


Fig. 5 - Lateral load-drift relations for PT connections without shear reinforcement

Note: 1 kip = 4.45 kN

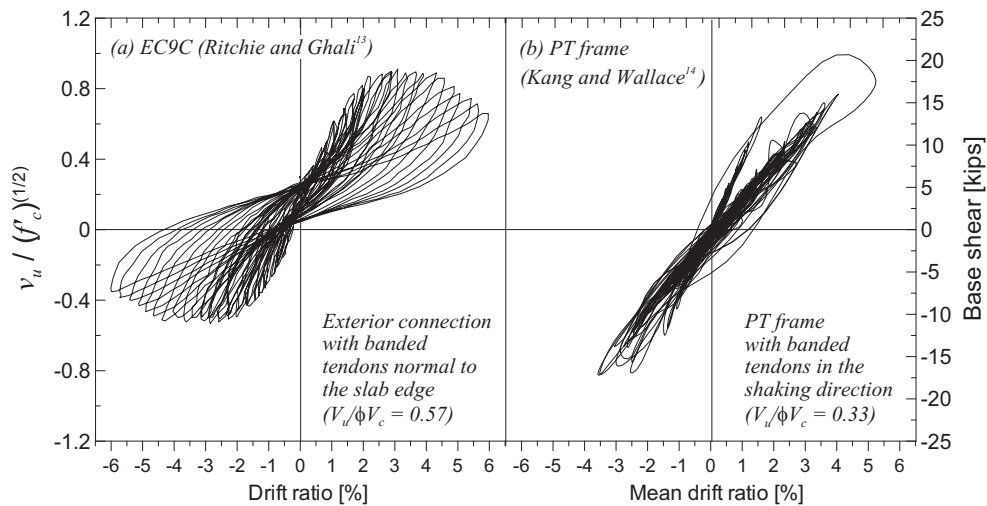


Fig. 6 - Lateral load-drift relations for PT connection and frame with shear reinforcement (Note that  $v_u$  is the shear stress on the critical perimeter based on the ACI eccentric shear stress model, and that  $1\sqrt{f'_c}$  psi =  $0.083\sqrt{f'_c}$  MPa and 1 kip = 4.445 kN)

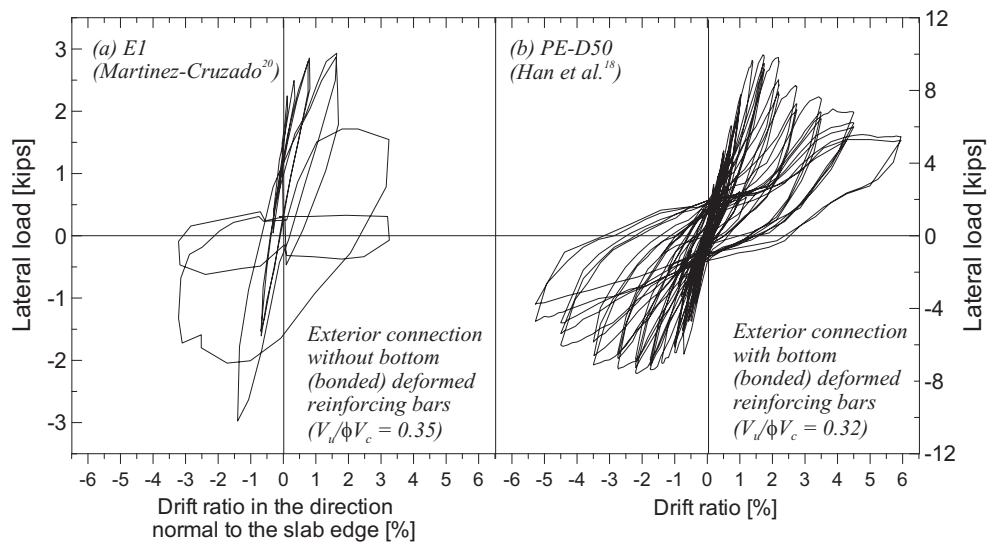


Fig. 7 - Comparison of lateral load-drift relations between PT connections with and without bottom bonded reinforcement Note: 1 kip = 4.45 kN

nections without bonded bottom reinforcement (e.g., Martinez-Cruzado,<sup>20</sup> Qaisrani<sup>21</sup>), punching failures occurred with little residual lateral strength (Fig. 7(a)). By contrast connections with bonded bottom reinforcement showed more energy dissipation, particularly at large drifts (e.g., considerable bottom rebar yielding; Kang and Wallace;<sup>14</sup> also as shown in Fig. 7(b); Han et al.<sup>17</sup>). In particular, Han et al.<sup>17,18</sup> investigated the necessity for, and the required quantity of, bonded bottom bars for PT interior and exterior connections. The test data indicate that moment reversal occurred at lateral drift ratios of approxi-

mately 0.5% and that bonded bottom reinforcement, placed according to ACI 318-05,<sup>1</sup> Section 7.13.2.5 and ACI 352.1R-89<sup>9</sup> Section 5.3 (i.e., the so-called structural integrity requirement), yielded at lateral drift ratios of between 2.2 and 3.5%. Based on these results, bonded bottom reinforcement could be beneficially provided for PT connections of non-participating frames where moment reversal is likely to occur. Note that this suggestion is not for the purpose of structural integrity, but rather for limiting cracking at moment reversal. Currently the Post-Tensioning Manual<sup>11</sup> (Section 6.4.2.2) only requires at least

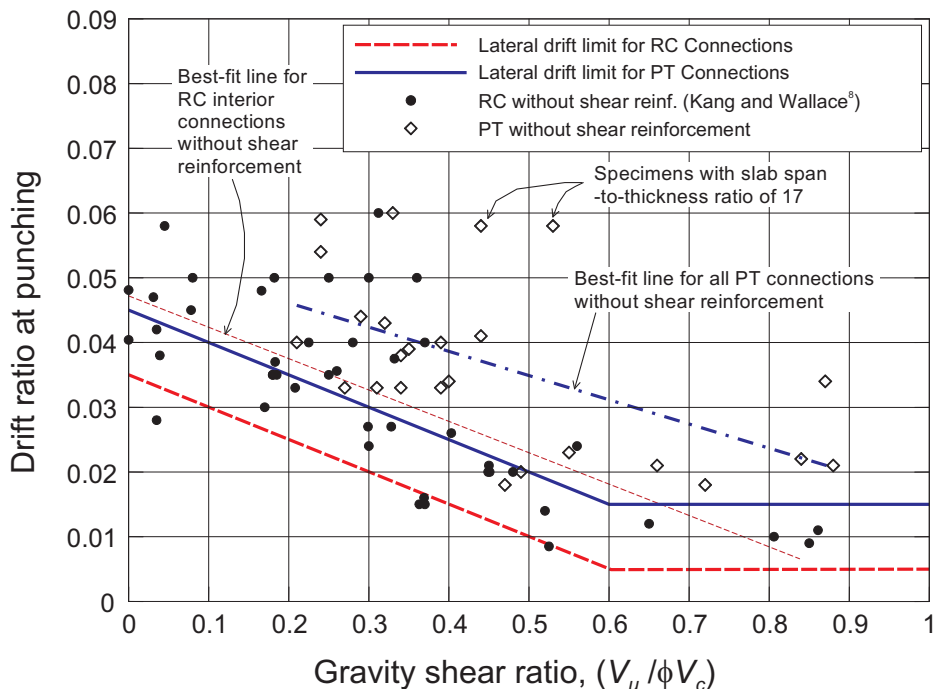


Fig. 8 - Comparison of drift limits with conventionally reinforced and post-tensioned slab-column connection test data, where  $V_c$  is defined in accordance with ACI 318-05, Eq. (11-33) through (11-36)

two post-tensioning tendons passing through the column core in each direction for structural integrity.

Based on the preceding review, a new bi-linear relation, as illustrated in Fig. 8 and as defined by Eq. (1), is proposed for the drift limit (drift ratio “DR”) above which the use of shear reinforcement should be required for PT slab-column connections that are part of non-participating frames subjected to the design-basis earthquake (DBE).

$$DR = \begin{cases} 0.045 - 0.05 VR & [\text{for } 0 \leq VR < 0.6] \\ 0.015 & [\text{for } 0.6 \leq VR \leq 1.0] \end{cases} \quad (1)$$

where VR is the gravity shear ratio, defined as

$$VR = \frac{V_u}{\phi V_c} \quad (2)$$

and where  $V_u$  is determined by the load combinations specified in ACI 318-05,<sup>1</sup> Section 21.11.5,  $\phi = 0.75$  per ACI 318-05<sup>1</sup> Section 9.3.2.3, and  $V_c$  is the punching shear strength of the post-tensioned connection,  $(\beta_p \sqrt{f'_c} + 0.3f_{pc})b_o d$  (lbs).

This new limit is nearly a lower bound estimate of the drift capacity at punching for all gravity shear ratios and for all connection types tested. Only two of the 39 test results fall slightly below the proposed relationship. If the design story drift ratio under the DBE exceeds the lateral drift capacity, DR, given by Eq. (1), then minimum shear reinforcement should be provided per Section 21.11.5 of ACI 318-05,<sup>1</sup> or the connection should be redesigned.

The alternative approach described in Section 21.11.5(a) of ACI 318-05 would be to develop a detailed model of the slab-column frame and subject it to the design lateral drift demand in order to calculate the connection shear stress demand due to  $V_u$  and the induced unbalanced moment under the design drift demand. For this approach, the potential for shear strength degradation due to inelastic deformation reversals should be considered when comparing the shear stress demand with the punching shear capacity. This could perhaps be addressed by use of  $\phi = 0.60$  for the shear strength per Section 9.3.4(a) of ACI 318-05.<sup>1</sup>

Based on the experimental data that meet a 1.5% drift limit (Fig. 8), the maximum allowable factored gravity shear force for post-tensioned connections that are part of intermediate moment frames (ACI 318-05,<sup>1</sup> Section 21.12.6.8) could be increased from the current  $0.4 \phi V_c$  up to at least  $0.6 \phi V_c$ . Further, this limitation could be waived if the story drift ratio does not exceed the drift limit of Eq. 1.

## PUNCHING SHEAR STRENGTH UNDER GRAVITY AND LATERAL LOADS

As an alternative to checking the drift limit, punching shear strengths for post-tensioned connections under gravity loads and lateral deformations can be checked against the shear stresses due to direct shear and moment transfer at all critical sections that may result in punching failures. The punching shear strength of a post-tensioned connection without shear reinforcement is defined per Section 11.12.2.2 of ACI 318-05<sup>1</sup> and Section 5.4.3 of the Post-Tensioning Manual.<sup>11</sup> The eccentric shear stress model is typically used for the shear design of the connection as recommended by Commentary Section 11.12.6.2 of ACI 318-05<sup>1</sup> and Section 5.4.3 of the Post-Tensioning Manual.<sup>11</sup>

Experimental databases for the shear strength of PT connections subjected to gravity loading or both gravity and lateral loading were recently assembled by Silva et al.<sup>24</sup> and Han et al.<sup>17,18</sup> The reported test results indicate that current ACI 318-05<sup>1</sup> provisions give conservative strength results for both interior and exterior post-tensioned connections without shear reinforcement (Fig. 9). In particular, it is recommended that the expression for  $V_c$  in Eq. (11-36) of ACI 318-05<sup>1</sup> be applicable to exterior connections provided that at least two tendons pass through the column core, they are normal to the discontinuous edge, and the remaining tendons in that direction are uniformly distributed across the width of the slab. Even for exterior connections with banded tendons normal to the discontinuous edge (Foutch et al.,<sup>15</sup> Martinez-Cruzado,<sup>20</sup> Han et al.<sup>17,18</sup>), a slight trend was observed such that the in-plane compressive stress  $f_{pc}$  increased the punching shear strength (Fig. 9).

While the limits of ACI 318-05<sup>1</sup> Section 11.12.2.2(a), (b), and (c) were ignored in developing the recommendations of this paper, it appears advisable, based on the reported behavior of the test specimens, that the design  $f_{pc}$  value should be between 125 and 500 psi and that the expression for  $V_c$  in Equation (11-36) be applicable to PT connections having  $\sqrt{f'_c}$  greater than 70 psi. On the other hand, there are no limitations on the values of  $\sqrt{f'_c}$  and  $f_{pc}$  in the Post-Tensioning Manual,<sup>11</sup> Section 5.4.3.

The ACI 318-05<sup>1</sup> nominal punching shear strength of a slab-column connection with shear reinforcement is a combination of the concrete and shear reinforcement capacities. The shear strength of the connection must be checked at all critical sections—for example,  $d/2$  from the column face within the shear-reinforced region (column critical section), and  $d/2$  outside the shear-reinforced region (outer critical section). The nominal shear strength  $V_n (= V_s + V_c)$  at the column critical section is defined per Section 11.12.3 of ACI 318-05<sup>1</sup> and Section 5.4 of the Post-Tensioning Manual,<sup>11</sup> where  $V_s$  is the nominal shear strength provided by shear reinforcement, and  $V_n$  and  $V_c$  shall not be taken greater than  $6\sqrt{f'_c} b_o d$  and  $2\sqrt{f'_c} b_o d$  (lbs), respectively. On the outer critical section,

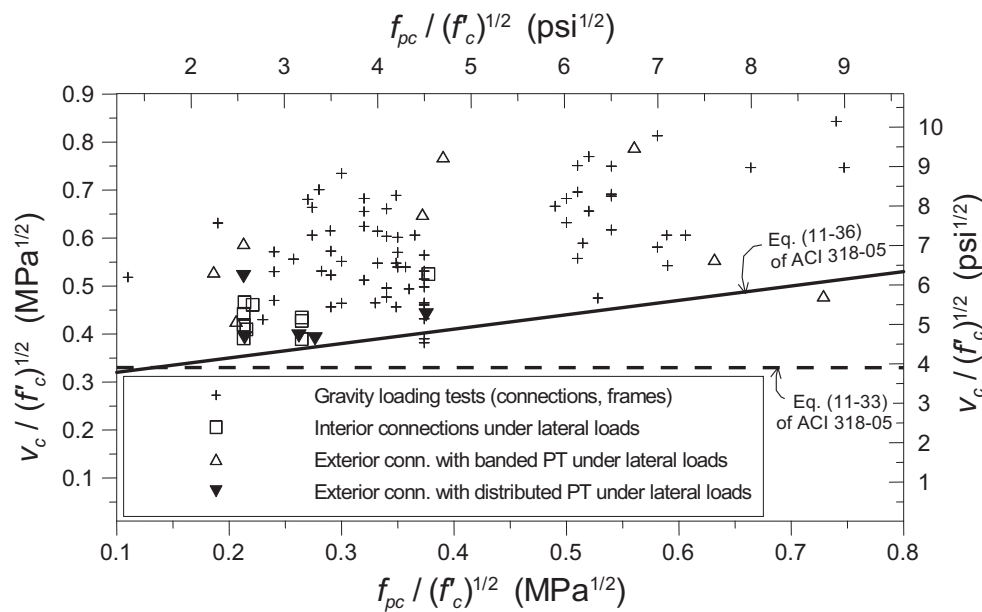


Fig. 9 - Punching shear strengths of PT connections and frames (from data compiled by Han et al.<sup>17,18</sup>; and Silva et al.<sup>24</sup>)

the concrete shear strength  $V_c$  shall not be taken greater than  $2\sqrt{f'_c} b_o d$  (lbs). Calculations required for the outer critical section are essentially the same as those for the column critical section, except for the change in the geometry of the critical section. Results for monotonic to reversed cyclic tests of PT slabs with headed studs and hairpin welded stirrups (Shatila,<sup>19</sup> Ritchie and Ghali,<sup>13</sup> Gayed and Ghali,<sup>16</sup> Saleh and Suaris<sup>25</sup>) suggest that the limiting values of  $V_n$  and  $V_c$  could be increased to  $8\sqrt{f'_c} b_o d$  and  $3\sqrt{f'_c} b_o d$  (lbs), respectively, possibly due to improved three-dimensional integrity provided by post-tensioning forces.

Current ACI 318-05,<sup>1</sup> Section 13.5.3.3 and Post-Tensioning Manual,<sup>11</sup> Section 5.4.3 do not allow redistribution of the moment being transferred (i.e., adjustments to  $\gamma_f$ ) for PT connections. Redistribution would affect the punching shear design and the slab flexure design at the connection. Given the equivalent or greater drift for PT connections compared with RC connections (as seen in Fig. 8), it appears reasonable to remove this restriction on  $\gamma_f$  adjustments for PT connections. Additional research, however, is needed to confirm this modification. It is also noted that for PT exterior connections with banded tendons perpendicular to the slab edge, the banded tendons provided sufficient membrane forces to move the torsional yield line outside the banded tendon region, or to suppress the torsional yield line completely (Fig. 4(c) and 4(d)). Thus, in this case it is reasonable that all reinforcement within the banded tendon region be considered effective in moment transfer if properly anchored (versus the ACI 318-05<sup>1</sup> defined effective transfer width of  $c_2 + 3h \leq c_2 + 2c_t$ , where  $c_t$  is the distance from the interior face of the col-

umn to the slab edge measured parallel to  $c_1$ , but not exceeding  $c_1$ , and  $c_1$  is the column dimension parallel to the loading direction).

#### SHEAR REINFORCEMENT DETAILS FOR EARTHQUAKE-RESISTANT DESIGN

For non-participating slab-column connections, (ACI 318-05,<sup>1</sup> Section 21.11.5), checking of the punching shear strength against eccentric shear demands due to earthquake-induced lateral displacement can be waived provided the design story drift ratio is less than the lateral drift capacity. Alternatively, minimum shear reinforcement should be provided such that its strength  $V_s$  is not less than  $3.5\sqrt{f'_c} b_o d$  (lbs) within a distance of  $4h$  away from, and perpendicular to, the column face. In the preceding section, a new drift limit for post-tensioned slab-column connections is suggested. It is also recommended that the lateral drift capacity check apply for intermediate slab-column connections, as an alternative to checking the shear stress demands.

Minimum distances for extending shear reinforcement from the column face are to ensure that punching failures do not occur at an outer critical section prior to punching failure at the column critical section, even for a worst case scenario, for connections with typical geometries and reinforcement details. For PT connections with shear reinforcement, the minimum length of shear reinforcement from the column face can be reduced from  $4h$  to  $3h$ . There was excellent performance of the PT connections with shear reinforcement when minimum lengths of  $1.9h$ ,

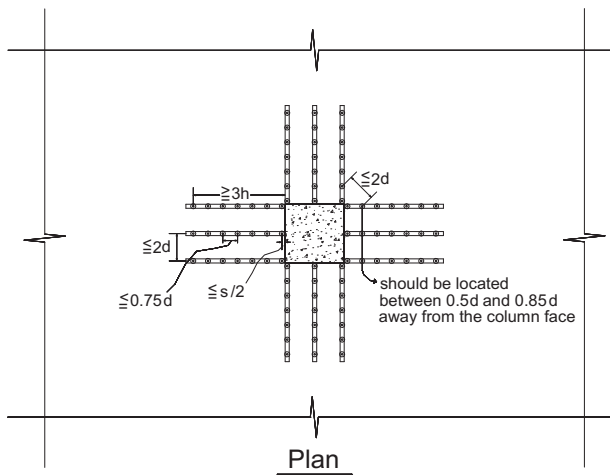


Fig. 10 - Shear reinforcement details for earthquake-resistant design (scaled)

2.25h, and 2.8h were used in the tests by Shatila,<sup>19</sup> by Kang and Wallace,<sup>14</sup> and by Ritchie and Ghali<sup>13</sup> and Gayed and Ghali,<sup>16</sup> respectively (e.g., Fig. 6(a) and 6(b)).

The ACI 318-05<sup>1</sup> code and commentary for Section 11.12.3 provide minimum requirements and recommendations for spacing and anchorage details of slab shear reinforcement. Based on the observed dynamic connection behavior (captured on video; Kang and Wallace<sup>8</sup>) and a review of prior studies by the authors, shear reinforcement for earthquake-resistant design is recommended to be detailed as follows: (1) the spacing between peripheral lines of shear reinforcement, *s*, should not exceed (1/2)*d* and (3/4)*d* for stirrups and headed shear studs, respectively; (2) the first peripheral line of shear reinforcement should be located within *s*/2 from the face of the column; (3) at least one peripheral line of shear reinforcement should be located between 0.5*d* and

0.85*d* from the face of the column; and (4) the distance between adjacent studs or stirrup legs along the first and second peripheral lines should not exceed 2*d* (Fig. 10). These shear reinforcement recommendations for earthquake-resistant design are fairly stringent so as to promote adequate shear strength at the interface between the slab and the column, and at the corner of the rectangular critical sections.

### ANCHORAGE OF COLUMN BARS IN ROOF SLAB-COLUMN JOINTS

Anchorage of column bars in roof slab-column joints is one of the reinforcement detailing issues not addressed in the ACI 318-05<sup>1</sup> provisions or any other recommendations. Nearly all of the laboratory tests for moment transfer at slab-column connections have been conducted using specimens with continuous columns extending above and below the slab. In the few related experiments that have been made on roof-type joints (e.g., Nilsson<sup>26</sup>), it has been apparent that anchoring the column reinforcing steel in the slab can be a problem.

Although roof beam-column joints should have the column hook tail extensions oriented to confine the core of the column (i.e., hook bent inward towards the joint), turning the tail extension inward can create severe congestion inside a “slab-column” joint and lead to poor compaction of the concrete in that area. Therefore, based on the views of the authors, the following details for roof slab-column joints are recommended: (1) use of 90 degree hooks for the column bars, with the tail extensions turned out into the slab (Fig. 11); (2) placement of the slab top bars above the hooks and tail extensions of the column bars; and (3) use of shear (double-headed studs) reinforcement (Fig. 12), as opposed to drop panels. The slab top bars placed above the column hooks and passing through the column in both directions will help prevent the hooked column bars from

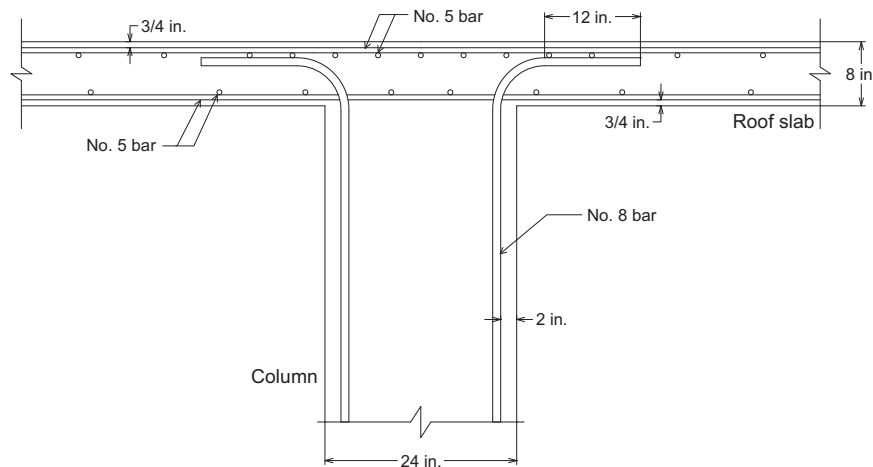


Fig. 11 - An example of details of column bar anchorage in roof slab-column joints (scaled)



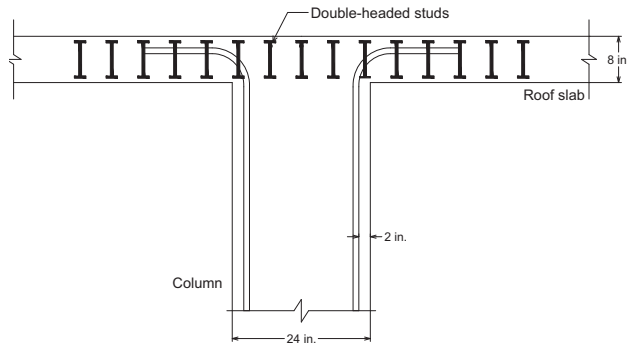


Fig. 12 - An example of use of double-headed studs to improve joint ductility (scaled)

breaking through the top surface of the slab in an earthquake, as well as provide restraint to the bending action of the column bars. Alternatively, column stubs can be provided above the roof joint for anchoring column hooked bars (e.g., Kang and Wallace<sup>14</sup>; Fig. 4(c)). Use of headed column reinforcement can also be a potential solution to the anchorage problem. However, experimental work should be carried out to validate this possibility.

For roof PT connections, there may be similar conditions and even worse congestion problems. Therefore, the same details for the anchorage and confinement are recommended, except for ensuring that the column bar hooks should not obstruct the route of draped unbonded tendons. Despite the detailing recommendations outlined above, because the column bar anchorage may not be effective under cyclic loading, it is recommended that such slab-column connection joints be assumed to be a hinge for analysis and design calculations.

## SUMMARY AND RECOMMENDATIONS

A detailed review of existing experimental data on lateral load tests of post-tensioned (PT) slab-column connections was conducted. The following recommendations are made for connection design based on this review:

- 1) Because the drift capacities for PT connections are higher than those for RC connections, a new drift limit for PT connections that are part of non-participating frames is proposed. That capacity equals the larger of 0.015 and  $[0.045 - 0.05(V_u/\phi V_c)]$ . Alternatively, a certain amount of shear reinforcement should be required in the slab.
- 2) Based on the measured drift capacities of PT connections and frames without shear reinforcement, the maximum allowable factored gravity shear force for PT connections that are part of intermediate

moment frames could be  $0.6\phi V_c$ . Alternatively, the story drift ratio of the PT intermediate frames could be limited to the larger of 0.015 and  $[0.045 - 0.05(V_u/\phi V_c)]$ .

- 3) Use of shear reinforcement reduces the extent of punching damage and of post-punching strength degradation. Use of bottom bonded reinforcement increases the hysteretic energy dissipation under deformation reversals into the inelastic range. However, there is no evidence that the use of either type of reinforcement significantly improves the lateral drift capacity at punching.
- 4) Based on the reported behavior of the test specimens, it appears advisable that the design pre-stress  $f_{pc}$  should be between 125 and 500 psi and that the expression for  $V_c$  in Eq. (11-36) of ACI 318-05 should be applicable to exterior connections, provided that at least two tendons pass through the column core, and are normal to the discontinuous edge, and that the remaining tendons in that direction are uniformly distributed across the width of the slab.
- 5) Based on prior test results of PT connections under both gravity and lateral loads, the punching shear capacities  $V_c$  and  $V_n$  for PT connections with shear reinforcement can be increased to  $3\sqrt{f'_c} b_o d$  and  $8\sqrt{f'_c} b_o d$  (lbs), respectively.
- 6) For PT non-participating slab-column frames that do not meet the drift limit requirements proposed here, a minimum amount of shear reinforcement is suggested such that  $V_s$  is not less than  $3.5\sqrt{f'_c} b_o d$  (lbs) within a distance of  $3h$  away from, and perpendicular to, the column face, with certain seismic spacing requirements.
- 7) Roof slab-column joint details are recommended such that 90 degree hooks for the column bars be placed below the slab top bars, with the tail extensions turned out into the slab. In addition, and if necessary, double-headed studs as shear reinforcement or a column stub above the roof joint can be used.

## ACKNOWLEDGEMENT

The authors would like to thank other members of the Joint ACI-ASCE Committee 352, Joints and Connections in Monolithic Concrete Structures, for their constructive comments and suggestions regarding the content of this paper.

## REFERENCES

1. ACI Committee 318 (2005), *Building Code Requirements for Structural Concrete (ACI 318-05) and Commentary (318R-05)*, American Concrete Institute, Farmington Hills, MI, 2005, 430 pp.
2. Moehle, J.P. (1996), *Seismic Design Considerations for Flat-Plate Construction*, Mete A. Sozen Symposium...A Tribute From His Students (SP-162), J.K. Wight and M.E. Kreger, eds, American Concrete Institute, Farmington Hills, MI, 1996, pp. 1-34.
3. Megally, S.; and Ghali, A. (2000), *Punching Shear Design of Earthquake-Resistant Slab-Column Connections*, ACI Structural Journal, V. 97, No. 5, Sept.-Oct. 2000, pp. 720-730.
4. Hueste, M.B.D.; Lepage, A.; Browning, J.P.; and Wallace, J.W. (2007), *Performance-Based Seismic Design Criteria for Slab-Column Connections*, ACI Structural Journal, V. 104, No. 4, July-Aug. 2007, pp. 448-458.
5. Pan, A.D.; and Moehle, J.P. (1989), *Lateral Displacement Ductility of Reinforced Concrete Flat Plates*, ACI Structural Journal, V. 86, No. 3, May-June 1989, pp. 250-258.
6. Hueste, M.B.D.; and Wight, J.K. (1999), *Nonlinear Punching Shear Failure Model for Interior Slab-Column Connections*, Journal of Structural Engineering, V. 125, No. 9, Sep. 1999, pp. 997-1008.
7. Robertson, I.N.; Kawai, T.; Lee, J.; and Enomoto, B. (2002), *Cyclic Testing of Slab-Column Connections with Shear Reinforcement*, ACI Structural Journal, V. 99, No. 5, Sept.-Oct. 2002, pp. 605-613.
8. Kang, T.H.-K.; and Wallace, J.W. (2006), *Punching of Reinforced and Post-Tensioned Concrete Slab-Column Connections*, ACI Structural Journal, V. 103, No. 4, July-Aug. 2006, pp. 531-540.
9. Joint ACI-ASCE Committee 352 (2004), *Recommendations for Design of Slab-Column Connections in Monolithic Reinforced Concrete Structures (ACI 352.1R-89) (Reapproved 2004)*, American Concrete Institute, Farmington Hills, MI, 2004, 22 pp.
10. Pimanmas, A.; Warnitchai, P.; and Pongpornsup, S. (2004), *Seismic Performance of 3/5 Scaled Post-tensioned Interior Flat Slab-Column Connections*, Proceedings of the Asia Conference on Earthquake Engineering, Manila, Philippines, Mar. 2004, 9 pp.
11. PTI (2006), *Post-Tensioning Manual – Sixth Edition*, Post-Tensioning Institute, Phoenix, AZ, 2006.
12. Trongtham, N.; and Hawkins, N.M. (1977), *Moment Transfer to Columns in Unbonded Post-Tensioned Prestressed Concrete Slabs*, Report SM77-3, Department of Civil Engineering, University of Washington, Seattle, WA, 1977, 186 pp.
13. Ritchie, M.; and Ghali, A. (2005), *Seismic-Resistant Connections of Edge Columns with Prestressed Slabs*, ACI Structural Journal, V. 102, No. 2, Mar.-Apr. 2005, pp. 314-323.
14. Kang, T.H.-K.; and Wallace, J.W. (2005), *Dynamic Responses of Flat Plate Systems with Shear Reinforcement*, ACI Structural Journal, V. 102, No. 5, Sept.-Oct. 2005, pp. 763-773.
15. Foutch, D.A.; Gamble, W.L.; and Sunidja, H. (1990), *Tests of Post-Tensioned Concrete Slab-Edge Column Connections*, ACI Structural Journal, V. 87, No. 2, Mar.-Apr. 1990, pp. 167-179.
16. Gayed, R.B.; and Ghali, A. (2006), *Seismic-Resistant Joints of Interior Columns with Prestressed Slabs*, ACI Structural Journal, V. 103, No.5, Sept.-Oct. 2006, pp. 710-719.
17. Han, S.W.; Kee, S.-H.; Kang, T.H.-K.; Ha, S.-S.; Wallace, J.W.; and Lee, L.-H. (2006), *Cyclic Behaviour of Interior Post-Tensioned Flat Plate Connections*, Magazine of Concrete Research, Telford, V. 58, No. 10, Dec. 2006, pp. 699-711.
18. Han, S.W.; Kee, S.-H.; Park, Y.-M.; Lee, L.-H.; and Kang, T.H.-K. (2006), *Hysteretic Behavior of Exterior Post-Tensioned Flat Plate Connections*, Engineering Structures, V. 28, No. 14, Dec. 2006b, pp. 1983-1996.
19. Shatila, M. (1987), *Prestressed Concrete Slab-Edge Column Connection with Stud Shear Reinforcement*, MSc thesis, Department of Civil Engineering, University of Calgary, Calgary, AB, Canada, 1987, 203 pp.
20. Martinez-Cruzado, J.A. (1993), *Experimental Study of Post-Tensioned Flat Plate Exterior Slab-Column Connections Subjected to Gravity and Biaxial Loading*, PhD thesis, Department of Civil Engineering, University of California, Berkeley, CA, 1993, 378 pp.
21. Qaisrani, A.-N. (1993), *Interior Post-Tensioned Flat-Plate Connections Subjected to Vertical and Biaxial Lateral Loading*, PhD thesis, Department of Civil Engineering, University of California, Berkeley, CA, 1993, 303 pp.
22. Concrete International (2005), *Concrete Q & A – Checking Punching Shear Strength by the ACI Code*, Concrete International, V. 27, No. 11, Nov. 2005, pp. 76.

23. Kang, T.H.-K.; and Wallace, J.W. (2008), *Stresses in Unbonded Tendons of Post-Tensioned Flat Plate Systems under Dynamic Excitation*, Journal of the Post-Tensioning Institute, Vol. 6, No. 1, Feb. 2008.
24. Silva, R.J.C.; Regan, P.E.; and Guilherme, S.S.A.M. (2006), *Punching of Post-Tensioned Slabs – Tests and Codes*, ACI Structural Journal, V. 104, No. 2, Mar.-Apr. 2006, pp. 123-132.
25. Saleh, Z.A.; and Suaris, W. (2007), *Punching Shear Capacity of Post-Tensioning Slab with Hairpin Shaped Reinforcements*, Journal of the Post-Tensioning Institute, V. 5, No. 1, Jul. 2007, pp. 39-47.
26. Nilsson, I.H.E. (1973), *Reinforced Concrete Corners and Joints Subjected to Bending Moment*, Document D7:1973, National Swedish Building Research, Stockholm, Sweden, 1973, pp. 249.

#### CONVERSION FACTORS

1 in.	=	25.4 mm
1 psi	=	6895 N/m <sup>2</sup>
1 lb	=	4.45 N
1 kip	=	4.45 kN
1 kip-in.	=	0.113 kN-m
$\sqrt{f'_c}$ psi	=	$0.083\sqrt{f'_c}$ MPa

PTI member **Thomas H.-K. Kang** is an Assistant Professor of Civil Engineering at the University of Oklahoma, Norman, and a licensed P.E. in California. He is the Secretary of Joint ACI-ASCE Committee 352, Joints and Connections in Monolithic Concrete Structures, and is a member of ACI Committee 369, Seismic Repair and Rehabilitation; and the PTI Building Design Committee. His research interests include large-scale testing of reinforced and prestressed concrete structures, and nonlinear dynamic modeling of structural components and systems.

**Ian N. Robertson** is a Professor of Civil Engineering at the University of Hawaii at Manoa and 2008 president of the Structural Engineers Association of Hawaii. He is a member of Joint ACI-ASCE Committee 352, Joints and Connections in Monolithic Concrete Structures, and is a member of ACI Committee 209, Shrinkage and Creep. His research interests include the performance of reinforced and prestressed concrete structures subjected to extreme loading, and long-term effects, including creep, shrinkage and reinforcement corrosion.

**Neil M. Hawkins**, F.A.C.I., is a Professor Emeritus of Civil Engineering at the University of Illinois at Urbana-Champaign. He is on ACI 318, chairs its Task Group on Seismic Design of Piles, and is also a member of its subcommittees on Shear and Seismic Design. He is a member of Committees 215, Fatigue of Concrete; 408, Development and Splicing of Deformed Bars; 445, Shear and Torsion; 446, Fracture Mechanics; 550, Precast Concrete Structures; and ITG-5, Precast Shear Walls for High Seismic Applications. He chairs the concrete subcommittees of the Seismic Task Group of ASCE/SEI 7 on Minimum Design Loads for Buildings and that of the BSSC that develops the NEHRP Recommended Seismic Provisions for New Buildings. His primary interests are in the transfer of significant research advances into practice.

**James M. LaFave** is an Associate Professor of Civil Engineering at the University of Illinois at Urbana-Champaign and a licensed Professional Engineer. He is the Chair of Joint ACI-ASCE Committee 352, Joints and Connections in Monolithic Concrete Structures, and is a member of ACI Committees 374, Performance-Based Seismic Design of Concrete Buildings; 439, Steel Reinforcement; and E 802, Teaching Methods and Educational Materials. His research interests include earthquake-resistant design of reinforced concrete structures and durability of structural concrete.